



HAL
open science

Optimizing experimental parameters for tracking of diffusing particles

Christian L. Vestergaard

► **To cite this version:**

Christian L. Vestergaard. Optimizing experimental parameters for tracking of diffusing particles. 2015. hal-01144950v1

HAL Id: hal-01144950

<https://hal.science/hal-01144950v1>

Preprint submitted on 2 Nov 2015 (v1), last revised 10 Oct 2016 (v2)

HAL is a multi-disciplinary open access archive for the deposit and dissemination of scientific research documents, whether they are published or not. The documents may come from teaching and research institutions in France or abroad, or from public or private research centers.

L'archive ouverte pluridisciplinaire **HAL**, est destinée au dépôt et à la diffusion de documents scientifiques de niveau recherche, publiés ou non, émanant des établissements d'enseignement et de recherche français ou étrangers, des laboratoires publics ou privés.

Optimizing experimental parameters for tracking of diffusing particles

Christian L. Vestergaard*

Department of Micro- and Nanotechnology, Technical University of Denmark, Kgs. Lyngby, DK-2800, Denmark.
Aix Marseille Université, Université de Toulon, CNRS,
CPT, UMR 7332, 13288 Marseille, France (current address).

(Dated: April 22, 2015)

We describe how a single-particle tracking experiment should be designed in order for its recorded trajectories to contain the most information about a tracked particle's diffusion coefficient. The precision of estimators for the diffusion coefficient is affected by motion blur, limited photon statistics, and the length of recorded time-series. We demonstrate that precision is negligibly affected by motion blur in typical experiments, while optimizing photon counts and the number of recorded frames is the key to precision. Building on these results, we describe for a wide range of experimental scenarios how to choose experimental parameters in order to optimize the precision. Generally, one should choose quantity over quality: experiments should be designed to maximize the number of frames recorded in a time-series, even if this means lower information content in individual frames.

I. INTRODUCTION

Single-particle tracking using time-lapse photography [1, 2] enables investigation of diffusion of single molecules, e.g., proteins on cellular structures such as DNA [3] and microtubules [4], on cell membranes [1, 5], and inside cells [6, 7]. Diffusion is ubiquitous at the microscopic level and precise determination of diffusion coefficients is paramount for understanding many chemical and biological processes. Typical single-particle-tracking experiments consist in recording the photons emitted by a fluorescent particle (a fluorophore) using time-lapse photography, and determining the particle's positions from recorded images using a super-resolution technique [1, 2, 8, 9]. The number of photons emitted by a fluorophore is limited, and traditionally, tracked particles have been recorded by leaving the camera shutter open continuously to maximize the number of photons recorded by the camera. The time the camera's shutter stays open to take a single image, its *exposure time*, is then equal to the time elapsed between consecutive images, the *time-lapse* of recordings. The motion of the tracked particle during the time-lapse results in motion blur in the pictures (also referred to as *dynamic error*), while diffraction and limited photon statistics result in localization error (also referred to as *static error*) [9–11]. Additionally, the length of a time-series, i.e., the number of recorded positions, is usually limited, either due to bleaching of the fluorophore or to the tracked particle diffusing out of the field-of-view. All of the above adversely affect the precision of estimates of diffusion coefficients and make it important to get the most out of experimental data.

A typical experiment for tracking single diffusing particles can be divided into multiple steps (Fig. 1): (i) designing the experiment, e.g., choosing reagents, setting the video rate of the camera and the intensity of the illumination laser; (ii) carrying out the experiment, i.e.,

recording images of the fluorescent particles; (iii) treating images, localizing particles, and creating time-series of positions; (iv) estimating diffusion coefficients from the time-series. Optimal estimates of the particles' diffusion coefficients is obtained by optimizing each individual step. Recently, the questions of how to best localize and track single particles [2, 8, 9] and of how to optimally estimate diffusion coefficients from the resulting time-lapse-recorded trajectories has been addressed [11–14].

With (near) optimal localization methods and estimators of diffusion coefficients at hand, we can now address the first step in the workflow: how should experiments be designed in order for recorded trajectories to contain the most information about diffusion coefficients? One may turn several dials to influence the amount of information available for estimation of diffusion coefficients: One may adjust both the video rate of the camera and the photon emission rate of the tracked fluorophores. Furthermore, the motion blur in recorded images can be controlled by leaving the shutter open for only part of the time-lapse, following a given shutter sequence. The advent of stroboscopic tracking techniques [6], which synchronize illumination and recording of the sample, makes it possible to control the motion blur without sacrificing photon economy.

Recent studies have partly addressed the question, but a systematic investigation is lacking. It has namely been suggested that one may increase the precision of estimated diffusion coefficients by maximizing the motion blur using a double-pulse illumination sequence, i.e., short pulse-like illumination and recording of the sample at the very start and end of each time-lapse [11]. Another study has investigated the effect of adjusting several experimental parameters in more detail [13], though without explicitly considering the trade-off between the number of frames recorded (the time-series length) and the signal in each frame. It suggested that for time-independent illumination, the shutter should be left open during the whole time-lapse to maximize photon economy, and the number of photons recorded in an image

* cvestergaard@gmail.com

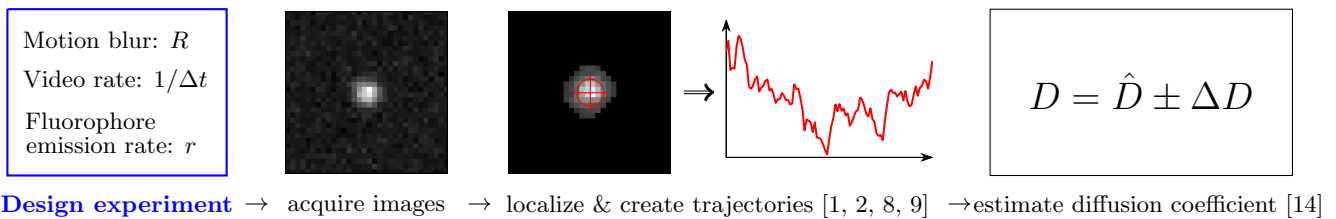


FIG. 1. Workflow for estimating diffusion coefficients from single-particle-tracking experiments. We are here concerned with optimizing the first step: how to choose experimental parameters (motion blur, video rate, and photon emission rate of the tracked fluorophore) for optimal precision of estimates of the diffusion coefficient of a tracked particle. The motion blur is characterized by a *motion blur coefficient*, $R \in (0, 1/4)$ [Eq. (8)] [11]. The motion blur coefficient, R , and video rate, $1/\Delta t$, may normally be controlled directly, while photon emission rate of the fluorophore, r , may be controlled indirectly, e.g., by varying the laser intensity or adding chemical reagents to the solution. Optimization of other steps in the workflow is addressed in the references given in the legends.

should be just enough to practically maximize the information content in individual recorded frames. These results relied on assumptions that neglected subtle but important details of localization of diffusing particles. The former study [11] neglected that motion blur increases the width of the measured photon distribution at the camera [the point-spread function (PSF)] increasing the localization error. The latter [13] took this effect into account, but neglected background noise, which is inevitable in experiment and leads to a non-linear dependence of the localization error on motion blur; this effect is especially important when motion blur or background noise is high.

We here perform a systematic analytical and numerical study of how to choose experimental parameters for tracking of diffusing particles in order to maximize the information in recorded time-series. We consider two different scenarios which cover the experimental situations usually encountered in single-particle tracking: (i) where the time that a particle can be followed, the *recording time*, t_{tot} , is the limiting factor; (ii) where the photostability of the fluorophore, and thus the total number of signal photons, P_{tot} , that can be recorded is the limiting factor. We show for both cases how to optimize experimental parameters.

In order to answer the question of how to optimally choose experimental parameters for tracking of diffusing particles, we first need to study how motion blur and limited photon statistics influence the precision of optimal estimators of the diffusion coefficient. This is done in Secs. II and III, while Sec. IV applies these results to optimize experimental design.

Specifically, we investigate in Sec. II how limited photon statistics and motion blur affect the precision of commonly used localization methods. We review analytical results for the localization error that results from localizing a stationary particle. We then derive an expression for the average measured width of the PSF of a diffusing particle. Using this, we give an approximate expression for the localization error for a diffusing particle, valid when the mean diffusion length of the tracked particle is smaller than the width of the PSF of a stationary fluo-

rophore.

In Sec. III, we next review the statistics of time-lapse recorded data of a diffusing particle and use the results of the previous section to investigate how motion blur affects the precision of estimates of diffusion coefficients. We show that recording using the double pulse illumination sequence suggested in [11] tends to *increase* the error on diffusion coefficient estimates. However, when recording with time-independent illumination and leaving the shutter open continuously, the effect of motion blur is negligible for relevant values of experimental parameters, and focus should be on photon economy.

Building on these results, we finally show in Sec. IV how experiments should be optimized for maximum precision in the different experimental scenarios. In general, experiments should be designed to maximize the number of frames recorded, not the number of photons recorded per frame—only enough photons should be recorded such that localization does not fail. This maximizes the information content in the time-series and, in turn, the precision of estimated diffusion coefficients. The reason for this is that the precision of estimated diffusion coefficient increases as the square root of the number of recorded positions, while the decrease in the signal in individual frames does not influence the precision as much, except for very low signal where the two effects balance and the precision approaches its maximum.

A short appendix details how the precision of the various localization methods was characterized on Monte Carlo generated data.

II. LOCALIZING A DIFFUSING PARTICLE

In this section results for localization in single-particle tracking are reviewed and the influence of motion blur and limited photon statistics is investigated. We consider in the following only diffusion in the image plane. However, for typical particle tracking experiments, where the focal plane is kept the same throughout the experiment (i.e., focus is not changed to follow an individual

particle), we show that diffusion along the optical axis effectively contributes to the localization error simply by a constant additive term and a slight change of the motion blur coefficient [9]. This means that conclusions drawn here for 2D diffusion in the image plane also hold for 3D diffusion.

In Subsec. A we review localization of stationary particles and give expressions for the localization error associated with different methods. In Subsec. B we then derive an expression for the average width of the PSF of a diffusing particle for a general time-dependent shutter/illumination sequence. Finally, in Subsec. C, following the approach of [9], we use this result to extend the expressions for localization error to tracking of a diffusing particle. We compare the analytical results to Monte Carlo simulations and discuss the limits of the analytical approach.

A. Localization error for a fixed particle

The diffraction-limited PSF emitted by a freely rotating fluorescent molecule or a fluorescent bead recorded by a CMOS, CCD, or EMCCD camera is well approximated by a two-dimensional (2D) Gaussian function plus a constant background term [8]. For an isolated fluorophore of this kind with fixed position, fitting a 2D Gaussian plus a constant to the measured PSF allows us to estimate the position of the molecule more precisely than the width of the PSF. This is done optimally using the maximum likelihood estimator with Gaussian PSF (MLEwG) [8].

When the fluorescent particle's position is estimated using MLEwG it leads to a white-noise localization error with variance

$$\sigma_0^2 = \frac{F s_a^2}{P} \left(1 + \int_0^t \frac{\ln t}{1 + P a^2 t / (2\pi b^2 s_a^2)} dt \right)^{-1}, \quad (1)$$

for camera pixel width a , background photon count b^2 , total number of signal photons P , and effective PSF width $s_a^2 = s_0^2 + a^2/12$, where s_0 is the width of the PSF of a stationary fluorophore (typically $s_0 \approx 100$ – 150 nm [8, 9]). Here F is a factor describing excess noise in the camera: for a CCD or CMOS camera there is no excess noise and $F = 1$, while for an EMCCD camera electron multiplication leads to excess noise and $F = 2$.

The particle's position is often estimated by a least squares fit to the PSF—the Gaussian Mask Estimator (GME) [8]—or by determining the centroid of an area containing the PSF [9]. This results in a localization error with variance of the form [8, 9]

$$\sigma_0^2 = \frac{F s_a^2}{P} \left(\alpha + \beta \frac{2\pi b^2 s_a^2}{P a^2} \right), \quad (2)$$

where for GME $\alpha = 16/9$ and $\beta = 4$ [8], and for the centroid method $\alpha = 1$ and $\beta = 81/8$ when all pixels contributing to the PSF, and only these, have been included [9].

In the following we assume a linear relation between the amplitude of the background photon noise and the amplitude of the peak signal, i.e. $b^2 = q P a^2 / (2\pi s_a^2)$. Here q is the proportionality factor, which we shall refer to as the background-to-signal ratio. This accounts for both the background noise from autofluorescence and other fluorophores, as well as the contribution from the power-law tails of the true PSF [8]. The second can normally be absorbed in the background, but is seen when the background noise is low. The background-to-signal ratio q is typically of the order of one [8]. Using this definition of q , Eqs. (1) and (2) can be simplified: for MLEwG,

$$\sigma_0^2 = \frac{F s_a^2}{P} \left(1 + \int_0^t \frac{\ln t}{1 + t/q} dt \right)^{-1}, \quad (3)$$

and for GME or the centroid method,

$$\sigma_0^2 = \frac{F s_a^2}{P} (\alpha + \beta q). \quad (4)$$

In practice, when localizing a particle, one must first define a general region of interest (ROI) containing only the particle one wants to track. The choice of the ROI naturally affects the localization precision. The centroid method is particularly sensitive to this as including pixels which only contain background noise increases its error—the error continues to increase as more background pixels are included, diverging with the size of the ROI. GME and MLEwG, which fit the background noise as a constant offset, are less sensitive to background noise and thus to the size of the ROI. However, errors in correctly defining the ROI will adversely affect the performance of any localization method. Common procedures for defining the ROI involve a thresholding procedure [15], which only retains pixels with a photon count over a certain threshold and selects the largest cluster of such pixels as the ROI (Appendix). Correctly determining the ROI notably becomes difficult when signal photons are few.

We investigate in Fig. 2 how limited photon statistics affects the precision of the various localization methods in practice. The localization error is approximately proportional to $1/\sqrt{P}$ as predicted theoretically; for low P , it is somewhat higher in practice than theoretical results, which can be expected due to difficulties in defining the ROI and since Eqs. (3) and (4) are only strictly valid in the limit of large P .

We also see that the localization procedures sometimes simply fail to localize the particle (defined as when the error between estimated and true average positions is larger than three times the PSF width, $3s_a$) [16]. This fraction, ϵ , is zero for large P and increases abruptly for $P < P_{\min} \approx 100$. Here P_{\min} then defines the minimal number of photons needed for reliable localization, which in general depends on the localization procedure used. More advanced methods, notably methods using the preceding and following positions of a tracked particle to localize it [2], may decrease P_{\min} . Conversely, excess noise, which is not present in the simulations of

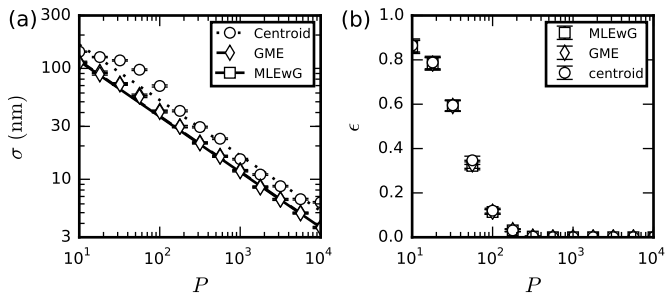


FIG. 2. Performance of the various methods when localizing a static particle as function of the number of signal photons recorded, P . (a) Amplitude of localization errors of the various methods. (b) Fraction of cases where the localization procedure fails to localize the particle (defined as when the error between estimated and true average positions is larger than $3s_a$) [16].

Fig. 2, will tend to make ROI determination harder since it increases the variance of the background noise by a factor two. The overall shape of ϵ as function of P does not change, however: it is practically zero for large P and approaches one for small P . (See [2] for a thorough review of single-particle-tracking algorithms and comparison of their performance.)

B. Motion blur increases the width of the point-spread function

Now consider a fluorescent particle diffusing in the image plane. A fluorescent molecule emits photons with a fixed rate in a Poisson process. The photons are collected by the camera during a time-lapse Δt to create an image.

The diffusion length during a time-lapse, $\sqrt{2D\Delta t}$, is in general much smaller than the microscope's field-of-view. So we can assume that the dispersion of photons in the microscope is independent of the particle's position during the time-lapse Δt . This means that we can for the moment neglect diffraction and finite photon statistics. The effect of these are added later by convoluting the PSF of a stationary particle with the distribution of positions of the diffusing particle during the time-lapse. Furthermore, since the motion in the x - and y -directions of a particle diffusing in a homogeneous medium are independent, the motion along the two axes are identical and can be treated separately as one-dimensional (1D) problems. The result derived here is thus valid for both one- and two-dimensional diffusion, and in the following derivation we consider 1D diffusion only. Finally, since the photon emission process is independent of the particle's position, we do not need to take fluctuations in photon emission into account to derive the average width of the measured PSF.

We can thus split the time-lapse Δt into M points in time, $\tau_0, \tau_1, \dots, \tau_M$. At each time-point τ_i the generic illumination function I_i determines whether the particle's

position is recorded. (It can be considered as an indicator function, which is equal to 1 for time-points when the particle's position is recorded and is equal to zero otherwise.) We then get a razor-sharp image of the tracked particle's trajectory. The width δx of the distribution of recorded positions around the center of mass of such a trajectory is given by

$$(\delta x)^2 = \frac{1}{P} \sum_{i=1}^M I_i (x_i - \bar{x})^2, \quad (5)$$

where $P = \sum_i I_i$ is the total number of photons recorded and \bar{x} is the average position. Since P is large (typically of the order of 100 or more) the sum is well approximated by an integral, and the expected value of $(\delta x)^2$ is

$$\langle (\delta x)^2 \rangle = \int_0^{\Delta t} I(t) \langle [x(t) - \bar{x}]^2 \rangle dt, \quad (6)$$

where $\bar{x} = \int_0^{\Delta t} I(t)x(t)dt$, and I is the continuous illumination function, which satisfies $\int_0^{\Delta t} I(t)dt = 1$. We insert the expected value $\langle x(t)x(t') \rangle = 2D \min(t, t')$ into Eq. (6) and perform partial integration to get

$$\begin{aligned} \langle (\delta x)^2 \rangle &= 2D \left(\int_0^{\Delta t} I(t)dt - \int_0^{\Delta t} I(t) \int_0^{\Delta t} I(t') \min(t, t') dt' dt \right) \\ &= 2D \left(- \int_0^{\Delta t} I(t) \int_0^t I(t') t' dt' dt + \int_0^{\Delta t} I(t) S(t) t dt \right) \\ &= 2D \int_0^{\Delta t} S(t) [1 - S(t)] dt \\ &= 2RD\Delta t, \end{aligned} \quad (7)$$

where R is the motion blur coefficient, defined by

$$R = \frac{1}{\Delta t} \int_0^{\Delta t} S(t) [1 - S(t)] dt, \quad (8)$$

and $S(t) = \int_0^t I(t') dt'$ [11]. Important special cases are: (i) Constant (time-independent) illumination, used in experiments without stroboscopic setup to maximize photon count—here $R = 1/6$; (ii) an instantaneous illumination pulse, which minimizes motion blur—here $R = 0$; (iii) the double pulse illumination suggested in [11], which maximizes the motion blur—here $R = 1/4$.

Since the photon emission process is independent of the particle's position, the average width of the Gaussian part of the measured PSF (the measured distribution minus the constant background) is

$$s^2 = s_a^2 + 2RD\Delta t. \quad (9)$$

For a constant illumination function (i.e. time-independent illumination and continuously open shutter) Eq. (9) simplifies to the result found in [9]. This differs from the result found in [12, 17] since the initial positions of the particle at the start of each time-frame in those

studies were implicitly assumed to be known, which is not the case in actual particle-tracking experiments.

When tracking particles undergoing 3D diffusion, e.g., using confocal microscopy, particles diffuse in and out of focus, increasing the width of the measured PSF. Following the approach of Deschout et al. [9, Supporting Material], we may use Eq. (8) to extend their result for the average width of the measured PSF emitted by a fluorescent particle undergoing both in-plane and out-of-plane diffusion,

$$s^2 = s_a^2 + 2RD\Delta t + s_0^2(z_{\text{lim}}^2 + 2RD\Delta t)/z_0^2 \\ = [1 + z_{\text{lim}}^2/(3z_0^2)]s_0^2 + 2R(1 + s_0^2/z_0^2)D\Delta t. \quad (10)$$

Here $z_0 = 4\pi ns_0^2/\lambda \approx 4s_0$, with numerical aperture of the objective n and photon wavelength λ , and z_{lim} is the distance from the focal plane where the particle becomes undetectable. Diffusion along the optical axis simply changes the effective stationary PSF width and slightly changes the motion blur coefficient, i.e., by approximately $1/16 \approx 6\%$. Thus, it does not qualitatively alter the results derived below. We thus consider only diffusion in the image plane in the following, but note that conclusions found here also apply to 3D diffusion.

Examples of measured PSFs of a particle diffusing in the image plane obtained from Monte Carlo simulations are shown in Fig. 3.

C. Localization error for a diffusing particle

Finally, we use the result derived above to extend expressions for the localization error presented in Sec. II A to localization of diffusing particles.

Following the same mean-field approximation used in [9, 13], we assume that the effect of motion blur on localization error is found simply replacing by s_a^2 by s^2 [Eq. (9)] in Eqs. (1)–(4) [Fig. 4(a)–(c)], e.g., for GME or centroid localization,

$$\sigma^2 = \frac{F(s_a^2 + 2RD\Delta t)}{P} \left[\alpha + \beta q \left(1 + \frac{2RD\Delta t}{s_a^2} \right) \right]. \quad (11)$$

Equation (11) shows that background noise leads to a faster-than-linear increase in the localization error as function of the motion blur.

The above result assumes a symmetrical PSF. However, since diffusion is not a stationary process, the contribution to the measured photon distribution from the diffusive movement is only symmetrical on average, not in a single image. This means that we can expect the analytical result to break down when motion blur becomes large enough to make the individual PSF significantly asymmetrical. In practice, for continuously open shutter, the theoretical result agrees well with numerical simulations when the diffusion length during a time-lapse is smaller than s_a^2 , i.e., when $\sqrt{2RD\Delta t}/s_a < 1/\sqrt{6}$ [Fig. 4(a)–(c)]. For experiments using the double-pulse

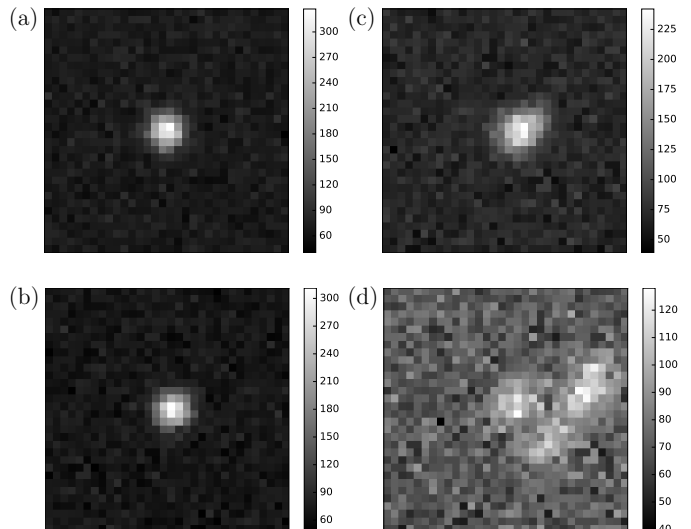


FIG. 3. Monte Carlo simulated images of measured PSFs emitted by stationary and diffusing fluorescent point-like particles at low background-noise conditions. (a) Stationary particle. (b) Particle diffusing in the image plane with mean diffusion length equal to the width of the PSF of a stationary particle, $\sqrt{2D\Delta t} = s_a$. (c) Diffusing particle with $\sqrt{2D\Delta t} = \sqrt{10}s_a$. (d) Diffusing particle with $\sqrt{2D\Delta t} = 10s_a$. In all plots, the total number of photons emitted by the particle is $P = 10\,000$, the background-to-signal ratio is $q = 0.1$, the pixel size is $a = 100$ nm, and the width of the stationary PSF is $s_a = 150$ nm. Note that the amplitude of the background noise is the same in the four panels, the difference in scale makes it appear higher in panels (c) and (d).

illumination sequence to maximize motion blur, the measured PSF is more asymmetrical, and the localization error is in practice higher than theoretically predicted even for modest motion blur. For low motion blur, the MLEwg and GME estimators are slightly more precise than the centroid estimator. For high motion blur, errors in ROI determination dominates the localization error, and all three estimators perform equivalently. Furthermore, high motion blur, especially when photon count is low, significantly increases the fraction of particles that are not correctly localized [Fig. 4(d)–(f)].

III. PRECISION OF ESTIMATORS OF THE DIFFUSION COEFFICIENT FROM A SINGLE TRAJECTORY

In this section we build on the results of the previous section to investigate how the precision of estimators of diffusion coefficients depend on experimental parameters. In Subsec. A we review the statistics of time-lapse recorded time-series of diffusing particles and define the parameters that determine the precision of estimators of diffusion coefficients. In Subsec. B we introduce the Cramér-Rao lower bound (CRB) which limits the precision of any unbiased estimator of the diffusion

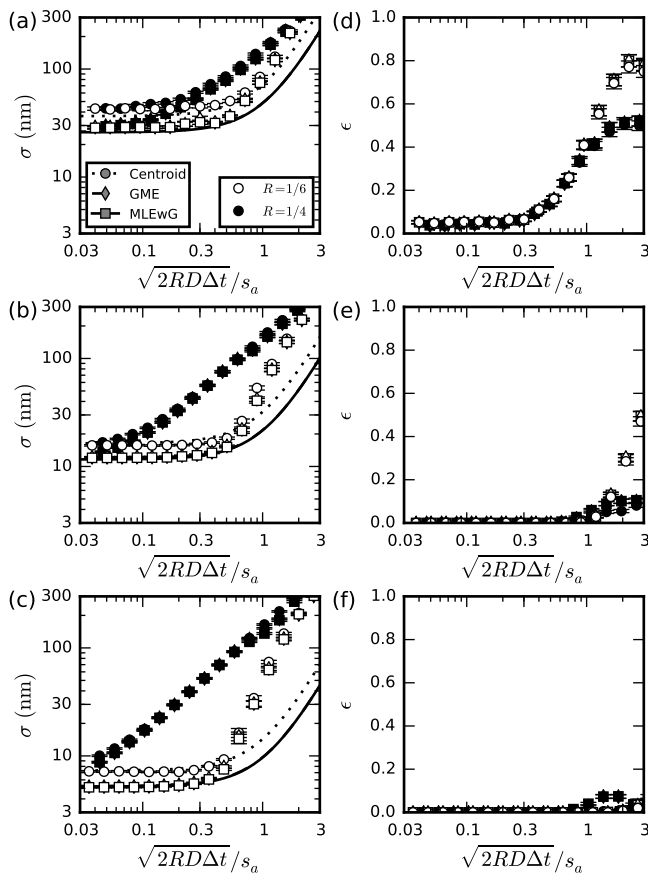


FIG. 4. (a)–(c) Amplitude of localization errors, σ , and (d)–(f) fraction of incorrectly localized particles as a function of normalized motion blur $\sqrt{2RD\Delta t}/s_a$. (The localization is considered to have failed if the error between the estimated and true average positions is higher than $3s = 3\sqrt{s_a^2 + 2RD\Delta t}$) [16] Lines mark theoretical errors [Eqs. (1)–(4)] and symbols mark mean errors (\pm s.e.m.) averaged over 1 000 MC simulations. The number signal photons per image are (a),(d) 200, (b),(e) 1000, and (c),(f) 5000. The width of the stationary PSF is $s_a = 150$ nm, the background-to-signal ratio is $q = 1$, and the results are for 2D diffusion in the image plane.

coefficient—it thus defines the precision of optimal estimators. In Subsec. C we investigate how the CRB depends on experimental parameters.

A. Statistics of recorded trajectories

In a single-particle-tracking experiment a time-series of $N + 1$ positions ($\mathbf{r}_0, \mathbf{r}_1, \dots, \mathbf{r}_N$) of a particle diffusing in d dimensions is determined with localization errors of amplitude σ from images recorded with time-lapse Δt . We define the set of N single-time-lapse displacements ($\Delta \mathbf{r}_1, \dots, \Delta \mathbf{r}_N$), given by $\Delta \mathbf{r}_n = \mathbf{r}_n - \mathbf{r}_{n-1}$. These displacements are Gaussian distributed with mean zero and

covariance [11]

$$\langle |\Delta \mathbf{r}_n|^2 \rangle = 2dD\Delta t + 2d(\sigma^2 - 2RD\Delta t) \quad (12a)$$

$$\langle \Delta \mathbf{r}_n \cdot \Delta \mathbf{r}_{n+1} \rangle = -d(\sigma^2 - 2RD\Delta t) \quad (12b)$$

$$\langle \Delta \mathbf{r}_m \cdot \Delta \mathbf{r}_n \rangle = 0 \quad \text{for } |n - m| > 1. \quad (12c)$$

We define the signal-to-noise ratio (SNR) as the mean diffusion length $\sqrt{2dD\Delta t}$ of a particle during one time-lapse divided by the mean contribution $\sqrt{2d}\sigma$ of the localization error to the measured displacement,

$$\text{SNR} = \frac{\sqrt{D\Delta t}}{\sigma}. \quad (13)$$

This SNR, along with the motion blur coefficient R , the time-series length N , and the dimension d , determines the precision of any estimator of D . Since the SNR itself depends on F , q , P , the ratio $\sqrt{2D\Delta t}/s_a$, and R , the precision of estimates of D is completely determined by seven parameters: (i) the ratio of the diffusion length to the PSF width, $\sqrt{2D\Delta t}/s_a$, (ii) the excess noise factor, F , (iii) the number of signal photons recorded per image, P , (iv) the background-to-signal ratio in images, q , (v) the motion blur coefficient, R , (vi) the number $N + 1$ of frames in the recorded time-series or, equivalently, the time-series length, N , and (vii) the dimension of the recorded time-series, d .

For diffusion in an isotropic medium, the influence of d is trivial, the variance of estimates of diffusion coefficients simply scales as $\propto 1/d$; we thus consider here only $d = 2$, but note that conclusions do not depend on d . Excess and background noise, quantified here by F and q , influence the precision of particle localization and thus the precision of estimated diffusion coefficients. However, since they do not change with Δt , P , R , and N , changing their values does not qualitatively change the results, and thus neither the conclusions presented in this manuscript. We fix in the following $F = 1$, corresponding to CDD or CMOS cameras, and $q = 1$, corresponding to typical background noise in experiment (other values of q are considered in Supplemental Fig. 2) [18]. The parameters we can control in an experiment are typically: $\sqrt{2D\Delta t}/s_a$ (through Δt , where $\sqrt{2D\Delta t}/s_a \propto \sqrt{\Delta t}$), P (through both Δt and the photon emission rate, r , where $P \propto \Delta t$ and $P \propto r$), R (by engineering the shutter/illumination sequence), and N (through Δt , where $N \propto 1/\Delta t$).

B. Precision of optimal estimators for the diffusion coefficient

One can construct estimators of the diffusion coefficient D and the variance σ^2 of the localization error based on a measured time-series (see e.g. [11, 13, 14]). We want such an estimator to be as accurate as possible, preferably unbiased. That is, an estimator of D should on average give the true value of D . Furthermore, we

want the estimator to be as precise as possible. The precision of any unbiased estimator of D is bounded by the information limit, the Cramér-Rao bound (CRB).

An estimator which is unbiased and obtains the CRB is considered optimal—the MLE [11, 13, 14] does this asymptotically (for $N \rightarrow \infty$), and a simple covariance-based estimator (CVE) does this for $\text{SNR} > 1$ and all N [14]. The commonly used least-squares fitting to measured mean-squared displacements (e.g., as described in [19]) is suboptimal and its use should be avoided (for a complete discussion see [14]).

Technically, the CRB is a lower bound on the variance of any unbiased estimator of the set (D, σ^2) —or of D alone if σ^2 has been determined independently. The CRB is defined as \mathcal{I}^{-1} , where \mathcal{I} is the Fisher information. When both D and σ^2 must be estimated from the time-series, \mathcal{I} is a matrix given by

$$\mathcal{I} = d \begin{pmatrix} \sum_{k=1}^N \frac{1}{\psi_k^2} \left(\frac{\partial \psi_k}{\partial D} \right)^2 & \sum_{k=1}^N \frac{1}{\psi_k^2} \frac{\partial \psi_k}{\partial D} \frac{\partial \psi_k}{\partial \sigma^2} \\ \sum_{k=1}^N \frac{1}{\psi_k^2} \frac{\partial \psi_k}{\partial D} \frac{\partial \psi_k}{\partial \sigma^2} & \sum_{k=1}^N \frac{1}{\psi_k^2} \left(\frac{\partial \psi_k}{\partial \sigma^2} \right)^2 \end{pmatrix} \quad (14)$$

with [13]

$$\psi_k = 2D\Delta t + 2 \left(1 - \cos \frac{\pi k}{N+1} \right) (\sigma^2 - 2RD\Delta t), \quad (15)$$

where ψ_k is the second moment of the normalized discrete sine transform of $(\Delta \mathbf{r}_1, \dots, \Delta \mathbf{r}_N)$.

It is usually possible to determine σ^2 independently, e.g., directly from the localization procedure as described in [8] when the motion blur is sufficiently small ($\sqrt{2D\Delta t} \leq s_a$), or by averaging over estimates of σ^2 obtained from multiple time-series recorded under the same experimental conditions as described in [14]. (Note that the first method relies on an approximately symmetric PSF and, if the shutter is held open continuously, thus that $\sqrt{2D\Delta t} < s_a$; the second method assumes that the time-series used in the average are recorded with the same localization error, and thus approximately the same motion blur.) With σ determined beforehand, all the information in the time-series is used to estimate D alone. This increases the precision of the estimate [14]. If σ^2 has been determined independently with high precision, and this information is used to estimate D from a time-series, the CRB on the variance of this estimate is

$$\mathcal{I}^{-1} = \frac{2D^2}{d} \left[\sum_{k=1}^N \left(\frac{1 - 2R \left(1 - \cos \frac{\pi k}{N+1} \right)}{1 + \left(\frac{\sigma^2}{D\Delta t} - 2R \right) \left(1 - \cos \frac{\pi k}{N+1} \right)} \right)^2 \right]^{-1} \quad (16)$$

Increasing N naturally decreases the CRB (CRB $\sim 1/\sqrt{N}$ for $N \gg 1$). Increasing the SNR also decreases the CRB: for low SNR the CRB approximately scales with the SNR as CRB $\sim 1/\sqrt{\text{SNR}}$ [11], while for high SNR the CRB approaches a constant value (Fig. 5); For $R = 0$, this asymptotic value for the CRB is equal to $\sqrt{6/(dN)}$ when both D and σ^2 are estimated from the

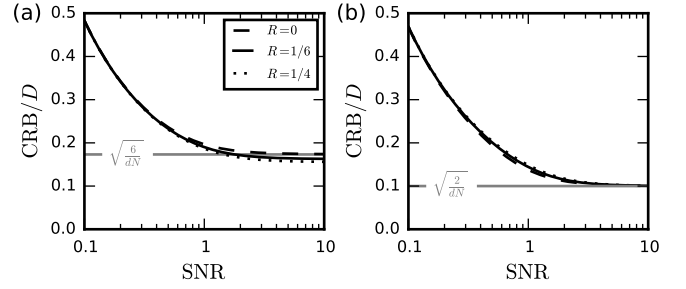


FIG. 5. Cramér-Rao bound (CRB) on the standard error of any unbiased estimator of the diffusion coefficient D as a function of the SNR ($\sqrt{D\Delta t}/\sigma$). Shown for different motion blur: no motion blur ($R = 0$), motion blur corresponding to continuously open shutter ($R = 1/6$), and maximal motion blur ($R = 1/4$). The CRB is measured in units of the true value of D . (a) If the amplitude of localization errors, σ , is unknown, increasing the motion blur while keeping the SNR constant lowers the standard error of an optimal estimator. (b) For known σ , the highest precision is obtained for minimal ($R = 0$) motion blur. Though in both cases (a,b) the difference in precision is small. Independent determination of σ lowers the standard error by up to a factor $\sqrt{3} \approx 1.7$ depending on the motion blur and the SNR. In both plots, results are for 2D diffusion and the length of the time-series is $N = 100$.

time-series [13], and it is equal to $\sqrt{2/(dN)}$ when σ^2 has been determined independently [14]. More surprisingly, when both D and σ^2 are estimated from a time-series, higher motion blur leads to a lower error [11]—if the SNR is kept the same. Conversely, if σ^2 has been determined independently, the CRB is lowest for minimal motion blur ($R = 0$).

C. Influence of motion blur

The surprising point that increasing the motion blur may decrease the error on estimated diffusion coefficients hinges on the implicit, yet crucial, assumption that changing the motion blur does not change the SNR. However, as we have seen in Sec. II, increasing the motion blur increases the localization error and consequently decreases the SNR; especially if one uses the double pulse illumination sequence to maximize R (Fig. 4). So, one should compare estimator precision, not for fixed SNR, but for fixed $\sqrt{2D\Delta t}/s_a$ (below, the time-series' length N , the signal photon count P , and the background noise b^2 are assumed to be unchanged when changing R). This reveals that while motion blur may theoretically increase precision of estimated diffusion coefficients, in practice, increasing R decreases the precision (Figs. 6 and 7).

For all $R > 0$, the CRB depends non-monotonously on $\sqrt{2D\Delta t}/s_a$ (Figs. 6 and 7): as $\sqrt{2D\Delta t}/s_a$ is increased, the CRB first decreases as the SNR increases; for intermediate $\sqrt{2D\Delta t}/s_a$, the CRB stays constant at its minimal value since further increase in the SNR does not in-

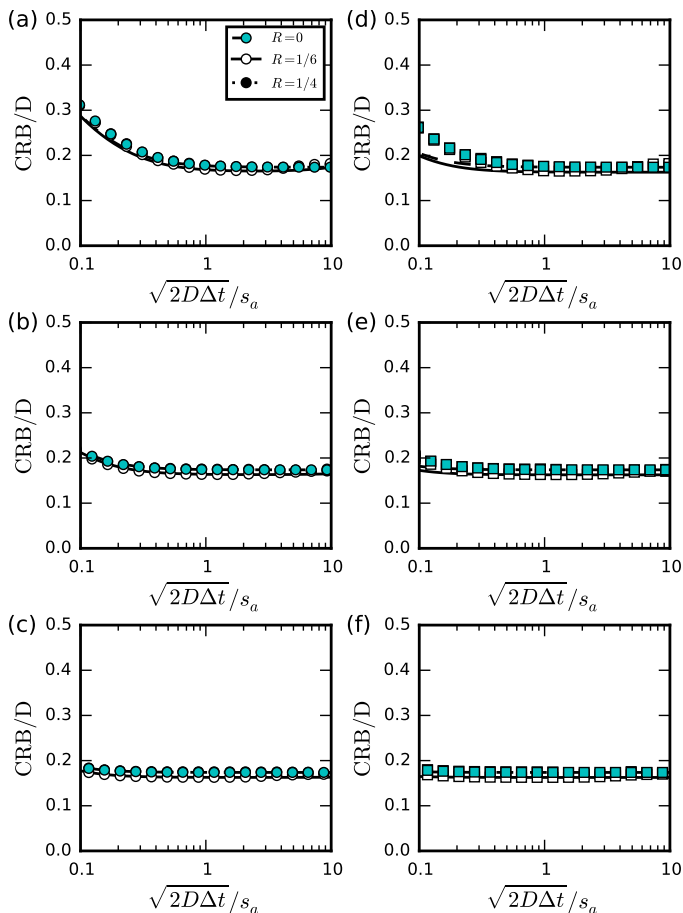


FIG. 6. Cramér-Rao bound (CRB) on the standard error of any unbiased estimator of the diffusion coefficient in the presence of motion blur when the amplitude of localization errors, σ , is unknown. Results for: no motion blur ($R = 0$), continuously open shutter ($R = 1/6$), and maximal motion blur ($R = 1/4$). The particle’s positions have been determined using the centroid method (a)–(c) or MLEwG (d)–(f). The number of signal photons per image is (a),(d) 200, (b),(e) 1000, and (c),(f) 5000. The motion blur coefficient slightly affects estimator precision, though in general the effect is negligible. For low $\sqrt{2D\Delta t}/s_a$ and P , and thus low SNR, the higher localization error of the centroid method leads to a somewhat higher CRB compared to MLEwG. In all plots results are shown for 2D diffusion, the background-to-signal ratio for photon count is $q = 1$, and the time-series length is $N = 100$. Note that D , Δt , and s_a do not need to be set to specific values to produce the plots as their ratio $\sqrt{2D\Delta t}/s_a$ fully determines precision.

fluence the CRB when the SNR is much larger than one; for high $\sqrt{2D\Delta t}/s_a$, the SNR decreases again since the localization error increases faster than linearly with the motion blur [Eq.(11)], eventually leading to an increase in the CRB. If one also considers that motion blur may induce failure of the localization procedure [Fig. 4(d)–(f)], which effectively reduces N , the increase in the CRB due to high motion blur is more dramatic [Supplemental Fig. 3] [18]. This result is in contrast to the result of [13],

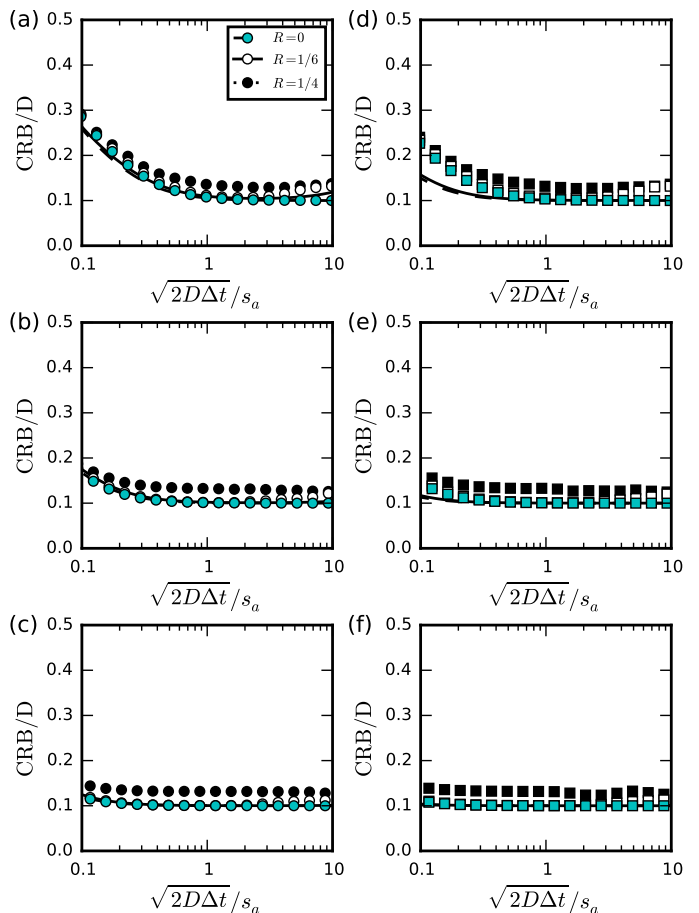


FIG. 7. Cramér-Rao bound (CRB) on the standard error of any unbiased estimator of the diffusion coefficient in the presence of motion blur when the amplitude of localization errors, σ , has been determined independently. Results for: no motion blur ($R = 0$), continuously open shutter ($R = 1/6$), and maximal motion blur ($R = 1/4$). The particle’s positions have been determined using the centroid method (a)–(c) or MLEwG (d)–(f). The number of signal photons per image is (a),(d) 200, (b),(e) 1000, and (c),(f) 5000. If σ has been determined independently increasing the motion blur coefficient always increases the estimation error, although only by a negligible amount, unless using the double pulse illumination sequence to maximize motion blur ($R = 1/4$). In all plots the tracked particle undergoes 2D diffusion, the background-to-signal ratio is $q = 1$, and the length of the time-series is $N = 100$.

where the omission of background noise led to the prediction that the SNR asymptotically approaches maximum as $\sqrt{2D\Delta t}/s_a$ is increased.

For moderate values of the motion blur, however, the CRB depends little on the motion blur coefficient. In particular, the difference between recording with instantaneous shutter ($R = 0$) and continuously open shutter ($R = 1/6$) is not significant as long as $\sqrt{2D\Delta t}/s_a < 1$. (For a typical value of the diffusion coefficient of $D \approx 1 \mu\text{m}^2\text{s}^{-1}$, this means that Δt should be smaller than $s_a^2/(2D) \approx 10$ ms; for different values of D , this

bound changes as $\propto 1/D$, e.g., for $D = 0.1 \mu\text{m}^2\text{s}^{-1}$: $\Delta t < 100$ ms, or for $D = 10 \mu\text{m}^2\text{s}^{-1}$: $\Delta t < 1$ ms.)

We have above assumed that P is not affected by engineering camera shutter and sample illumination in order to either increase or decrease motion blur (i.e. changing R from the value $R = 1/6$). In general, even if stroboscopic techniques are employed, this typically decreases P , and consequently increases the CRB.

In summary: as long as $\sqrt{2D\Delta t}/s_a < 1$, which is the relevant parameter range for optimizing the experiment (we shall see below), leaving the shutter open continuously gives the highest precision of estimated diffusion coefficients.

IV. OPTIMIZING EXPERIMENTAL DESIGN

Using the results derived in the preceding sections, we show how one should adjust the rate at which the tracked fluorescent particle emits photons, r , the time-lapse of recordings, Δt , and the motion blur coefficient, R , in order to maximize the information about the diffusion coefficient contained in a recorded time-series. We consider two different experimental scenarios, which together cover the experimental situations usually encountered in single-particle tracking. In Subsection A we consider the situation where the time that a particle can be followed, t_{tot} , is limited, e.g., since it diffuses out of the field of view of the microscope. In Subsection B we consider the situation where the photostability of the fluorescent particle limits the total number of photons that can be collected for a single trajectory, P_{tot} .

A. Limited experimental recording time

The total time a particle can be recorded $t_{\text{tot}} = (N+1)\Delta t$ may be limited by factors beyond experimental control. The particle may, e.g., detach from the substratum on which it diffuses, e.g. a cellular structure [20]. Or the particle may diffuse out of the microscope's field-of-view. The latter is typical for particles diffusing in three dimensions. If this happens on a time-scale which is shorter than the time-scale of bleaching, it is clear that one should maximize photon count by maximizing the rate r of photons collected from the fluorescent particle. This rate is limited in practice either by the photochemistry of the fluorescent particle or by the power of the available laser.

For a particle, which can be tracked for a time t_{tot} , the number of recorded signal photons per image is $P = r\Delta t$ and the length of the recorded time-series is $N = t_{\text{tot}}/\Delta t - 1$, assuming that one is able to determine the particle's position in all recorded images. Figure 8(b),(c) shows that the information content in a time-series is maximized by choosing Δt as small as possible, even though this leads to a smaller SNR in individual frames [Fig. 8(a)]. The reason for this is that

as long as $\text{SNR} > 1$, changing it does not change the CRB much [13], while the CRB always decreases with N as $\text{CRB} \sim 1/\sqrt{N}$ (Fig. 5); when $\text{SNR} \ll 1$, the CRB behaves as $\text{CRB} \sim 1/\sqrt{\text{SNR}}$ [Figs. 5(a),(b)], and since $\text{SNR} \sim 1/N$ [Fig. 8(a)], the CRB asymptotically approaches minimum as Δt is decreased towards zero.

In practice, since the number of signal photons recorded per time-lapse, P , decreases with Δt , the fraction of images for which the localization procedure fails, ϵ , increases as Δt is decreased [Fig. 8(d)]. (More performant tracking methods, which e.g. use the particle's estimated position in preceding and following images, may need fewer photons per image for correct localization; nonetheless, all localization methods, no matter how performant, eventually fail as P decreases.) Thus, the number of recorded positions is not $(N+1)$ when Δt is small, but rather $(1-\epsilon)(N+1)$. If the density of fluorescent particles is not too high, one is usually able to identify the full trajectory of a particle, even if some positions are missing. One may then fit the resulting time-series with an estimator that accounts correctly for missing positions [21]. In this case, Eqs. (14) and (16) with N replaced by $(1-\epsilon)N$ give lower bounds on the CRB, i.e., optimal estimators using this approach are at least this precise [grey symbols in Figs. 8(e),(f)]. If one is unable to identify the tracked particle again after a position is missing, one is then left with multiple shorter time-series. In this case, the CRB is given by $(\sum_{m=1}^M \mathcal{I}_m)^{-1}$ [black symbols in Figs. 8(e),(f)], where \mathcal{I}_m is the Fisher information for the m th individual contiguous time-series and M is the number of such time-series.

In both cases, the CRB initially decreases as Δt is decreased, following the theoretical prediction. When P becomes too small, the localization procedure starts to fail, and the CRB rapidly increases as Δt is decreased further since a smaller and smaller fraction of positions of the particle are found. The sweet spot, where the CRB is minimal—and precision is thus maximal—is found right before localization fails for a substantial fraction of the recorded images. Here the optimal choice of Δt is around $\Delta t = 10$ ms, corresponding to $P \approx P_{\text{min}} \approx 100$.

This result differs from the recommendation of [13], which suggested recording enough photons in each single image to ensure that $\text{SNR} > 1$, and then maximizing the number of frames recorded under this constraint.

Note finally, that a stroboscopic setup is of no practical use in this case, since the camera shutter must be kept open during the entire experiment to maximize photon count. Furthermore, since Δt should be chosen as short as possible, motion blur is usually not an issue and need not be taken explicitly into account in the localization procedure.

B. Limited photostability

Conversely, experiments may be limited by the photostability of the fluorescent particle, typical for proteins

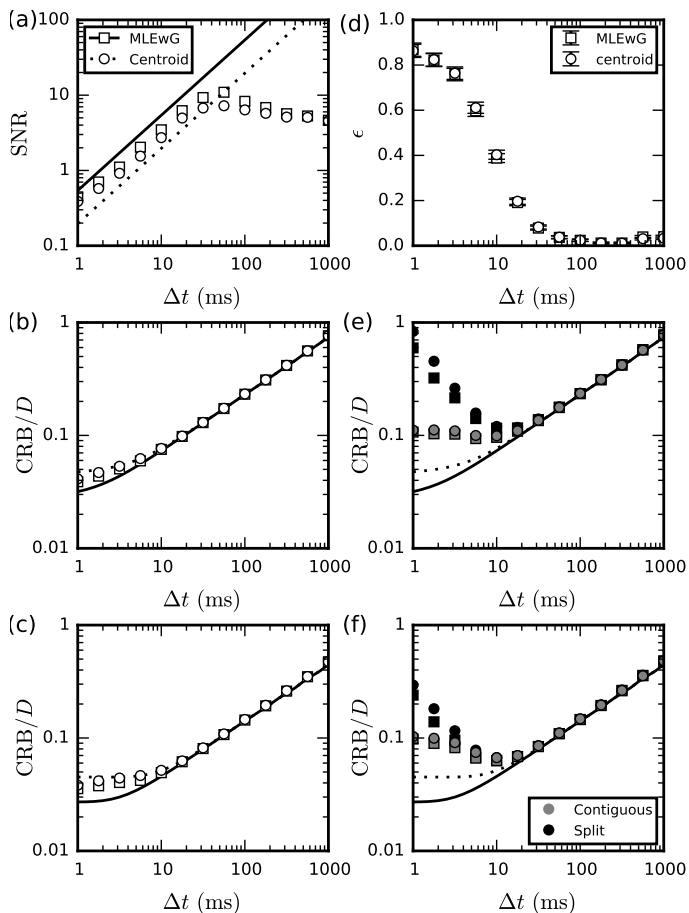


FIG. 8. Cramér-Rao bound (CRB) on the standard error of any unbiased estimator of the diffusion coefficient as function of time-lapse duration, Δt , for a time-series of limited recording time $t_{\text{tot}} = (N + 1)\Delta t$ (a) Signal-to-noise ratio (SNR) in a single frame as function of Δt . (b),(c) CRB as function of Δt when all $N + 1$ positions are found: (b) for unknown σ , (c) for independently determined σ . (d) Fraction, ϵ , of images for which localization fails as function of Δt . (e),(f) CRB as function of Δt when the particle is only localized for a fraction ϵ of the $N + 1$ images recorded, for the two different scenarios discussed in the main text: (i) where a contiguous trajectory can be constructed from the found positions (Contiguous), or (ii) where the particle cannot be reidentified after a position is missing and the trajectory is split into smaller time-series (Split); (e) for unknown σ , (f) for known σ . In all plots, the total recording time is $t_{\text{tot}} = 10$ s, the rate of photon emission of the fluorescent particle is $r = 10$ kHz, the width of the stationary PSF is $s_a = 150$ nm, the background-to-signal ratio in images is $q = 1$, the shutter is held continuously open ($R = 1/6$), and the particle undergoes 2D diffusion with diffusion coefficient $D = 1 \mu\text{m}^2\text{s}^{-1}$.

tagged with, e.g., GFP or an organic dye and bound in a lipid membrane [22]. In this case photon economy is paramount.

Let P_{tot} be the total number of photons emitted by the fluorescent particle before bleaching. Then $N = P_{\text{tot}}/P - 1$, with $P = r\Delta t$. From Fig. 5 we know that the

SNR needs only be slightly higher than one (or two if σ^2 is determined independently) for estimates of the diffusion coefficient from a given time-series to be maximally precise. We may thus simply choose Δt large enough that the SNR is always larger than one, i.e., $\Delta t > \sigma^2/(2D)$. In practice, we have $\sigma < s_a$ —higher error is indicative of failure of the localization procedure (Figs. 2 and 4)—and typically $\sigma \ll s_a$. So for typical values of physical parameters, $D = 1 \mu\text{m}^2\text{s}^{-1}$ and $s_a = 150$ nm, we may choose $\Delta t = 10$ ms $\approx s_a^2/(2D)$, i.e., a video-rate of 100 Hz; this way the motion blur is small enough to not influence localization error significantly, while the SNR is always higher than one for relevant values of P . (Note that the choice of Δt scales with $1/D$; for $D = 0.1 \mu\text{m}^2\text{s}^{-1}$ one should choose $\Delta t \approx 100$ ms, while for $D = 10 \mu\text{m}^2\text{s}^{-1}$ one should choose $\Delta t \approx 1$ ms, if possible.)

In general, as above, maximizing the number of images recorded is more important than the information in each image. The photon emission rate, r , should thus be adjusted to be as low as possible without the localization procedure failing (Fig. 9). This means choosing r such that the number of recorded signal photons per image is $P \approx P_{\text{min}}$ for optimal precision of estimates of the diffusion coefficients. Here $r \approx 10$ kHz is optimal, corresponding again to $P_{\text{min}} \approx 100$.

Note that, as above, a stroboscopic setup is typically of no practical relevance for optimizing the experiment. For fast diffusion proteins (e.g., $D \sim 10 \mu\text{m}^2\text{s}^{-1}$) one may not be able to choose Δt small enough ($\Delta t \approx 1$ ms), e.g., if the camera cannot record fast enough. Here a stroboscopic setup may be used. One should then simply maximize r and only let the shutter stay open for the short time-interval $P_{\text{min}}/r_{\text{max}}$ to minimize motion blur, while the time-lapse between measurements should be chosen to maximize the information content per image, i.e., letting $\Delta t > 4\sigma^2/(2D)$ (Fig. 5).

V. CONCLUSION

We have shown that one should choose quantity over quality when it comes to tracking diffusing particles. In general, experiments should be designed with focus on maximizing the number of frames recorded—the time-series length—even if this means a low SNR in individual frames. In particular, if the time a particle can be recorded is limited, e.g., by the particle diffusing out of the field-of-view, one should record the particle with a photon emission rate and a video rate that are as high as possible. If the experiment is limited by the fluorescent particle’s photostability, one should minimize the photon emission rate and record with a video rate that is slow enough to maximize the information content in each recorded frame yet fast enough to avoid the deleterious effects of motion blur—this is achieved by choosing the video rate such that the mean diffusion length per time lapse is equal to or slightly smaller than the PSF width of a stationary particle. In both cases, the fundamental

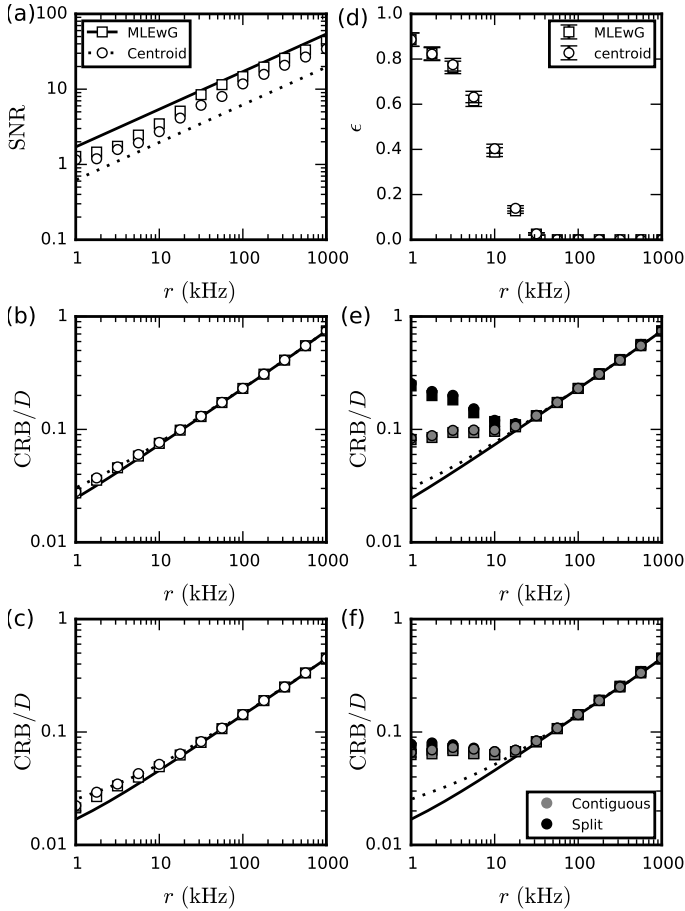


FIG. 9. Cramér-Rao bound (CRB) on the standard error of any unbiased estimator of the diffusion coefficient as function of photon emission rate, r , for a time-series whose length is limited by the total number of photons that can be recorded before the fluorophore bleaches, $P_{\text{tot}} = (N+1)P = (N+1)r\Delta t$ (a) Signal-to-noise ratio (SNR) in a single frame as function of r . (b),(c) CRB as function of r when the particle is localized in all $N + 1$ recorded images: (b) for unknown σ , (c) for known σ . (d) Fraction, ϵ , of images for which localization fails as function of r . (e),(f) CRB as function of r when the particle is only localized for a fraction ϵ of the $N + 1$ images recorded, for the two different scenarios discussed in the main text: (i) where a contiguous trajectory can be constructed from the found positions (Contiguous), or (ii) where the particle cannot be reidentified and the trajectory is split into smaller time-series (Split). (e) for unknown σ , (f) for known σ . In all plots, the total number of recorded photons is $P_{\text{tot}} = 10^5$, the time-lapse of recordings is $\Delta t = 10$ ms, the width of the stationary PSF is $s_a = 150$ nm, the background-to-signal ratio in images is $q = 1$, the shutter is held continuously open ($R = 1/6$), and the particle undergoes 2D diffusion with diffusion coefficient $D = 1 \mu\text{m}^2\text{s}^{-1}$.

limit on the precision is set by the minimal number, P_{min} , of signal photons needed in a single image for reliable localization.

The exact values of optimal Δt and r depend on experimental and physical parameters of the system un-

der study. However, the results presented in this paper may be used in one of two following ways in practice. (i) The quick and dirty way: according to whether recording time or photostability limits time-series length, fix either r or Δt and adjust the other to determine experimentally P_{min} as the point where localization starts to fail a substantial number of times (e.g. $\epsilon \approx 0.1$); the parameters giving this P_{min} are then approximately the optimal choice. (ii) The thorough way: if one wants to squeeze out every last drop of information from the experiment, one may follow the procedure described in the present paper to numerically find optimal experimental parameters for a given setup and localization method. This may even be done iteratively as D is estimated from experiments.

Similar procedures to the one presented here may be used to study how to optimize experimental parameters for tracking particles undergoing more complicated forms of motion, such as persistent random motion, active transport, or anomalous diffusion. Note that optimization in the definitive sense requires that an optimal estimator exists for the motion studied. While this often is not the case, at least not yet, one may still optimize experiments for a given (suboptimal) estimator of the motility parameters of the motion under study.

ACKNOWLEDGEMENTS

The author thanks R. Mastrandrea, J. Fournet, and A. Barrat for helpful discussions and H. Flyvbjerg, J. N. Pedersen, K. I. Mortensen, and M. Géniois for valuable suggestions and critical reading of the manuscript. This work was partly supported by the Human Frontier Science Program Research Grant GP0054/2009-C.

APPENDIX: NUMERICAL SIMULATIONS

The analytical results derived in the present paper rely on two simplifying assumptions. First, they neglect that in real-world tracking experiments, one must define a region of interest (ROI) containing the pixels which are used in fitting the tracked particle's position. The choice of ROI is particularly important for the centroid method where inclusion of background pixels increases the localization error—in the extreme case of an infinite ROI, the localization error of the centroid method is infinite. Second, the derivation of the localization error in presence of motion blur assumes an effectively symmetrical recorded PSF. We expect the first assumption to break down for low values of P and the second to break down for high motion blur.

To confirm the analytical approach for cases where we expect it to hold, and to investigate cases where it does not, we performed Monte Carlo simulations of a point-like diffusing fluorescent particle emitting photons recorded through a microscope by a CCD or CMOS camera. From such images we used an automated procedure

for selecting the ROI and fitting the PSF recorded inside this ROI in order to determine the precision of localization methods in practice.

Images were simulated using a continuous variant of the exact Gillespie algorithm [23], which uses that since photon emission is a Poisson process, the times elapsed between a particle emits two consecutive photons are exponentially distributed. The particle was started out at $(x_{\text{true}}, y_{\text{true}}) = (0, 0)$. An exponentially distributed waiting time until emission of the first photon was then drawn, $\tau_1 \sim \text{Exp}(r)$. [Here $\tau_1 \sim \text{Exp}(r)$ is short for τ_1 is exponentially distributed with mean $1/r$.] The displacement undergone by the particle in each perpendicular direction during the time-interval τ_1 was then drawn as $dx_{\text{true}}, dy_{\text{true}} \sim N(0, 2D\tau_1)$, i.e., both normally distributed with mean zero and variance $2D\tau_1$. The position of the particle at time $t = \tau_1$ was then $(x_{\text{true}}, y_{\text{true}}) = (dx_{\text{true}}, dy_{\text{true}})$; from this position the particle emitted a photon whose apparent position, as recorded by the camera, was equal to the particle's true position plus a photon noise term due to diffraction in the microscope, $\xi_x, \xi_y \sim N(0, 2s_a^2)$. A new waiting time $\tau_2 \sim \text{Exp}(r)$ was drawn; the particle's position was updated by adding $dx_{\text{true}}, dy_{\text{true}} \sim N(0, 2D\tau_2)$ to $(x_{\text{true}}, y_{\text{true}})$; the particle emitted a photon from its new position which was recorded with a photon noise term, $\xi_x, \xi_y \sim N(0, 2s_a^2)$. The procedure was repeated until $\sum_{i=1}^{P+1} \tau_i > \Delta t$, where the last photon (corresponding to $P+1$) was not recorded. The recorded photon positions were then compared to a 64×64 pixel grid of individual dimensions $a \times a = 100 \text{ nm} \times 100 \text{ nm}$ (the grid was large

enough that the particles did not diffuse out of the “camera” during the time-lapse); each position falling inside a given pixel added one to its count. Finally, Poisson distributed background noise was added to each pixel with mean $b^2 = qPa^2/(2\pi s_a^2)$.

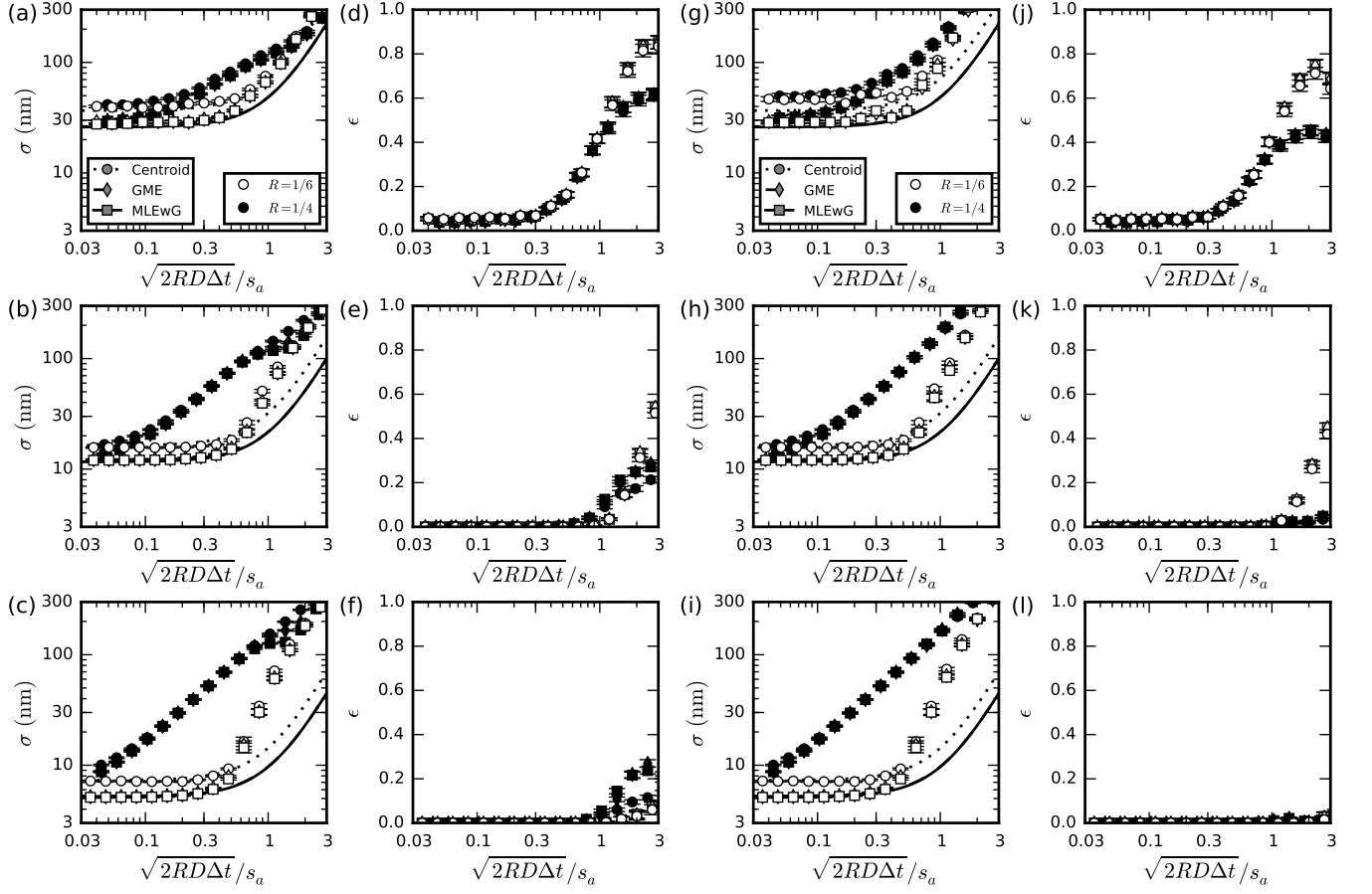
The resulting image, I , was then treated as follows to estimate the particle's average position. A thresholding procedure was performed which removed all pixels under a certain threshold equal to $n_{\text{thres}}b^2$, yielding a binary matrix A , with ones in pixels where the photon count was above the threshold and zeros where it was below. To remove single background pixels that were over the threshold due to random fluctuations, binary erosion of A by a 3×3 matrix was performed. The ROI was then expanded by a number n_{dilate} of successive binary dilations of A by a 3×3 matrix. The thresholds n_{thres} and n_{dilate} were chosen for the highest localization precision, and depended on P ; for GME and MLEwG, n_{dilate} needed only be large enough to include a substantial part of the PSF, while for the centroid method, n_{dilate} needed to be chosen as function of n_{thres} and P to maximize precision. The particle was then localized [8, 9] using only pixels of I that corresponded to non-zero entries of A . For the centroid method, fitting involved first subtracting the average background amplitude from all pixels [9]; the average background was estimated from pixels in a perimeter of three pixels around the ROI.

The above procedure was repeated 1 000 times for each set of parameter values in order to estimate the localization error of the various methods.

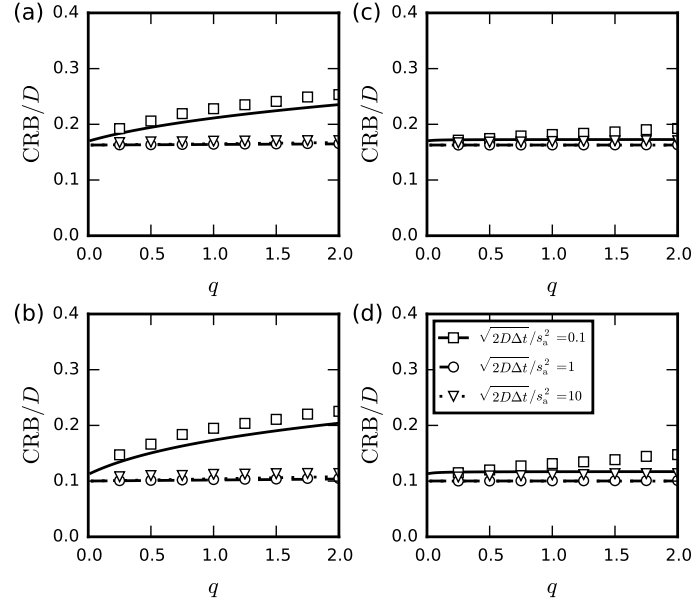
-
- [1] Sergé, A., Bertaux, N., Rigneault, H. & Marguet, D. Dynamic multiple-target tracing to probe spatiotemporal cartography of cell membranes. *Nat. Methods* **5**, 687–694 (2008).
- [2] Chenouard, N. *et al.* Objective comparison of particle tracking methods. *Nat. Methods* **11**, 281–289 (2014).
- [3] Tafvizi, A., Mirny, L. A. & van Oijen, A. M. Dancing on dna: kinetic aspects of search processes on dna. *Chemphyschem* **12**, 1481–1489 (2011).
- [4] Helenius, J., Brouhard, G., Kalaidzidis, Y., Diez, S. & Howard, J. The depolymerizing kinesin mcaK uses lattice diffusion to rapidly target microtubule ends. *Nature* **441**, 115–119 (2006).
- [5] Wieser, S. & Schütz, G. J. Tracking single molecules in the live cell plasma membrane—do's and don't's. *Methods* **46**, 131–140 (2008).
- [6] Elf, J., Li, G.-W. & Xie, X. S. Probing transcription factor dynamics at the single-molecule level in a living cell. *Science* **316**, 1191–1194 (2007).
- [7] Smith, M. B. *et al.* Interactive, computer-assisted tracking of speckle trajectories in fluorescence microscopy: application to actin polymerization and membrane fusion. *Biophys. J.* **101**, 1794–1804 (2011).
- [8] Mortensen, K. I., Churchman, L. S., Spudich, J. A. & Flyvbjerg, H. Optimized localization analysis for single-molecule tracking and super-resolution microscopy. *Nat. Methods* **7**, 377–381 (2010).
- [9] Deschout, H., Neyts, K. & Braeckmans, K. The influence of movement on the localization precision of sub-resolution particles in fluorescence microscopy. *J. Biophotonics* **5**, 97–109 (2012).
- [10] Savin, T. & Doyle, P. S. Static and dynamic errors in particle tracking microrheology. *Biophys. J.* **88**, 623–638 (2005).
- [11] Berglund, A. J. Statistics of camera-based single-particle tracking. *Phys. Rev. E* **82**, 011917 (2010).
- [12] Michalet, X. Mean square displacement analysis of single-particle trajectories with localization error: Brownian motion in an isotropic medium. *Phys. Rev. E* **82**, 041914 (2010).
- [13] Michalet, X. & Berglund, A. J. Optimal diffusion coefficient estimation in single-particle tracking. *Phys. Rev. E* **85**, 061916 (2012).
- [14] Vestergaard, C. L., Blainey, P. C. & Flyvbjerg, H. Optimal estimation of diffusion coefficients from single-particle trajectories. *Phys. Rev. E* **89**, 022726 (2014).
- [15] K. Braeckmans, J. D., D. Vercauteren & Smed, S. C. D. Single particle tracking. In Diaspro, A. (ed.) *Nanoscopy and Multidimensional Optical Fluorescence Microscopy* (Chapman and Hall/CRC 2010, 2010).

- [16] Note that while the choice of the threshold is arbitrary, its specific value does not influence the results qualitatively (see Supplemental Fig. 1) [18].
- [17] Schuster, J., Cichos, F. & von Borczyskowski, C. Diffusion measurements by single-molecule spot-size analysis. *J. Phys. Chem. A* **106** (22), 5403 (2002).
- [18] Supplemental figures are found at the end of the manuscript.
- [19] Qian, H., Sheetz, M. P. & Elson, E. L. Single particle tracking. analysis of diffusion and flow in two-dimensional systems. *Biophys. J.* **60**, 910–921 (1991).
- [20] Blainey, P. C., van Oijen, A. M., Banerjee, A., Verdine, G. L. & Xie, X. S. A base-excision dna-repair protein finds intrahelical lesion bases by fast sliding in contact with dna. *Proc. Natl. Acad. Sci. USA* **103**, 5752–5757 (2006).
- [21] Shuang, B. *et al.* Improved analysis for determining diffusion coefficients from short, single-molecule trajectories with photoblinking. *Langmuir* **29**, 228–234 (2013).
- [22] Domanov, Y. A. *et al.* Mobility in geometrically confined membranes. *Proc. Natl. Acad. Sci. USA* **108**, 12605–12610 (2011).
- [23] Gillespie, D. T. Exact stochastic simulation of coupled chemical reactions. *J. Phys. Chem.* **81**, 2340–2361 (1977).

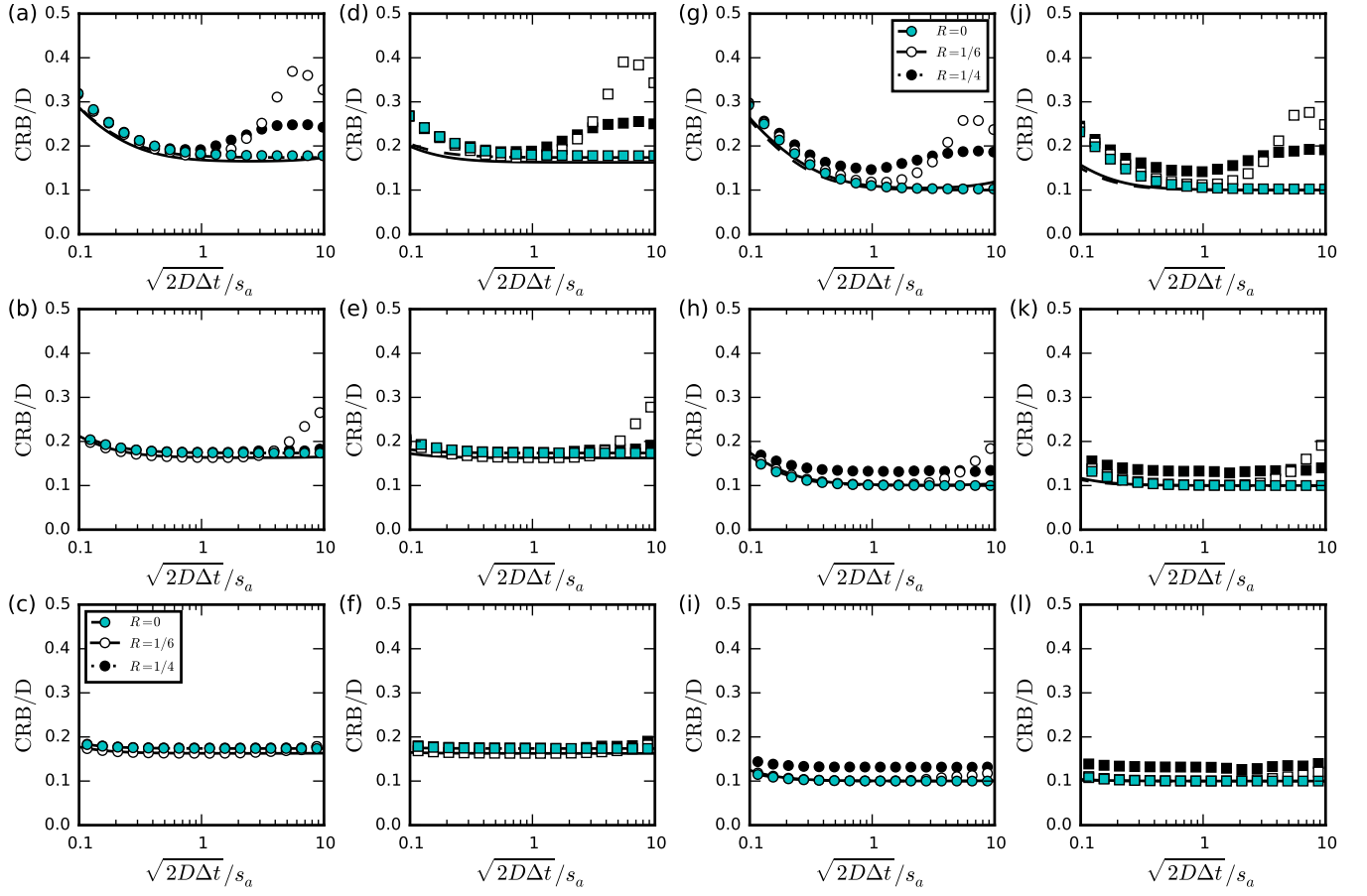
SUPPLEMENTAL FIGURES



Supplemental FIG. 1. Precision of localization methods as function of normalized motion blur, $\sqrt{2RD\Delta t}/s_a$, where localization is considered to have failed if the error between the estimated and true average positions is higher than (a)–(f) $2s = 2\sqrt{s_a^2 + 2RD\Delta t}$ or (g)–(l) $4s = 4\sqrt{s_a^2 + 2RD\Delta t}$. (a)–(c),(g)–(i) Amplitude of localization errors, σ , and (d)–(f),(j)–(l) fraction of incorrectly localized particles. Lines mark theoretical errors [Eqs. (1)–(4)] and symbols mark mean errors (\pm s.e.m.) averaged over 1000 MC simulations. The number signal photons per image are (a),(d) 200, (b),(e) 1000, and (c),(f) 5000. The width of the stationary PSF is $s_a = 150$ nm, the background-to-signal ratio is $q = 1$, and the results are for 2D diffusion in the image plane.



Supplemental FIG. 2. Cramér-Rao bound (CRB) on the standard error of any unbiased estimator of diffusion coefficients as a function of the background-to-signal ratio, q , for continuously open shutter ($R = 1/6$). (a),(b) For centroid localization, and (c),(d) for MLEwG localization. Increasing q , i.e., the background noise, adversely affects the precision of the centroid method and thus of diffusion coefficients estimated using it, though only for low $\sqrt{2D\Delta t}/s_a$; for low background the precision of the centroid method approaches that of MLEwG for all $\sqrt{2D\Delta t}/s_a$. Changing q does however not change the qualitative results presented in the Figs. 6–9. In all plots, the number of photons recorded per image is $P = 100$, the time-series length is $N = 100$, the stationary PSF width is $s_a = 150$ nm, and the particle diffuses in 2D.



Supplemental FIG. 3. Cramér-Rao bound (CRB) on the standard error of any unbiased estimator of the diffusion coefficient in the presence of motion blur where a fraction ϵ of the particle's positions are missing in the recorded time-series: (a)–(f) for unknown σ , (g)–(l) for known σ . The centroid method is used for localization in (a)–(c) and (g)–(i), while MLEwG is used in (d)–(f) and (j)–(l). The number of signal photons recorded per image is in (a),(d),(g),(j) 200, (b),(e),(h),(k) 1 000, and (c),(f),(i),(l) 5 000. In all plots results are shown for 2D diffusion, the background-to-signal ratio for photon count is $q = 1$, the number of recorded images is $N+1 = 101$, and the time-series length is $(1 - \epsilon)N$ [see Figs. 4(d)–(f) for corresponding values of ϵ].